Proceedings of Global Power and Propulsion Society
ISSN-Nr: 2504-4400
GPPS Hong Kong 2023
October 17-19, 2023
www.gpps.global

GPPS-TC-2023-0061

NUMERICAL MODELING OF TUBULAR REACTOR FOR CATALYTIC HYDROGEN GENERATION VIA AMMONIA DECOMPOSITION

Yashan Lin
Department of Applied Physics, The Hong Kong Polytechnic University
yashan.lin@connect.polyu.hk
Kowloon, Hong Kong, China

Zhengtong Li
Department of Aeronautical and Aviation Engineering, The Hong Kong Polytechnic University
zhengtong.li@connect.polyu.hk
Kowloon, Hong Kong, China

Zijian Zhang
Department of Aeronautical and Aviation Engineering, The Hong Kong Polytechnic University
zijian92.zhang@polyu.edu.hk
Kowloon, Hong Kong, China

Chih-Yung Wen
Department of Aeronautical and Aviation Engineering, The Hong Kong Polytechnic University
cywen@polyu.edu.hk
Kowloon, Hong Kong, China

Molly Meng-Jung Li
Department of Applied Physics, The Hong Kong Polytechnic University
molly.li@polyu.edu.hk
Kowloon, Hong Kong, China

ABSTRACT

Hydrogen (H_2) has been considered as a potential energy storage solution. However, the costly and technology-intensive infrastructure required for H_2 transportation and storage has hindered its widespread adoption. Ammonia (NH_3)-based energy storage system is thus emerging as a promising alternative for storing and producing H_2 without carbon emissions. However, the investigation of practical scale NH_3-to-H_2 reactor systems is strongly impeded by their labour-intensive and time-consuming features. Employing the computational fluid dynamic (CFD) simulation, we establish a two-dimensional model of a typical tubular fixed-bed reactor for NH_3 decomposition on our recently developed Ru/NiO composite catalyst. NH_3 conversion and H_2 production for fuel cell applications are theoretically and numerically predicted. Through a series of numerical simulations and experimental verifications, the underlying impact of catalyst porosity and inlet gas temperature on system performance is further investigated. The result shows that, at 500 °C, the NH_3 conversion can enhance from 13% to 49% with increasing porosity from 0.2 to 0.8, and from 47% to 86% by preheating inlet gas to wall temperatures. This work provides potential solutions for developing a scalable process to produce H_2, giving rise to a future reference and inspiration for clean energy development and applications.

INTRODUCTION

A significant number of nations and areas around the world have already mapped out a perspicuous path towards carbon neutrality to combat the global warming trend. In order to achieve a balance between a stable energy supply and environmental protection, the development of energy storage systems and energy generation technologies has been considered a vital mission of the times. The polymer electrolyte membrane (PEM) fuel cell is one of the most efficient and cleanest energy conversion systems and is expected to play a significant role in the development of future energy solutions (Giorgi et al., 2014). H_2 is the preferred fuel for PEM fuel cells without carbon emissions, as its electrochemical oxidation produces only water (H_2O). Even though the PEM fuel cell is an efficient and environmentally friendly technology, it is susceptible to impurities in the fuel. The reforming of hydrocarbon fuels is the primary source of H_2 gas, and low quantities of CO_x (5–10 ppm) can be poison to the fuel cell electrocatalysts and dramatically reduce the system efficiency. In addition, the difficulty in storing and transporting H_2 due to its flammability and extremely low volumetric energy density severely hindered the development and widespread commercial uses of PEM fuel cell technology.

Using non-carbon chemical H_2 carriers for the on-demand production of H_2 is an alternate method for solving these challenges associated with H_2 transport and storage. NH_3 has an admirable energy density (3000 Wh/kg) and H_2 content (17.8 wt%). Moreover, at 8 atm and room temperature, NH_3 is easily stored in the form of liquid, hence it can serve as a

crucial H_2 storage medium. In addition, the H_2 produced by the decomposition of NH_3 does not contain CO_x, and the unreacted NH_3 can be removed using an absorber unit. Consequently, the potential of NH_3 as a carbon-free H_2 transporter is quite attractive. The dehydrogenation of NH_3 produces a combination of H_2 and nitrogen (N_2) gas ($2\ NH_3 \rightarrow 3\ H_2 + N_2$) that can be utilized to directly power the current fuel cells. Thus, the thermal cracking of NH_3 to produce H_2 for fuel cells has been frequently studied in recent years (Chang et al., 2021).

Pourali et al. (2022) investigated eight process variables in NH_3 decomposition reaction using CFD simulation and suggested a suitable design, with a porosity of around 0.8 and pore diameters >1.5 mm of $Co_{0.5}Ce_{0.1}Al_{0.4}O$ catalyst, was optimal for constructing experimental prototypes. Takahashi et al. (2021) concluded that the relationship between the Ru/MgO catalyst-bed diameter (0.01-0.03 m) and flow rate (0.2-10 m^3/h) largely dominated the temperature distribution in the tubular reactor, and consequently the catalytic activity in H_2 production. They proposed that NH_3 treatment with 10 m^3/h at a space velocity (SV) = 15 000 h^{-1} in practical applications can be achieved by multiplexing 10 reactors with 1 m^3/h per single reactor. Deng et al. (2020) investigated the impact of catalyst diameter (0.5-2 mm), porosity (0.2-0.8) and fluid flow modes (one side in & one side out, middle in & both sides out, and both sides in & middle out). They concluded that the requirements for reactor performance improvements were as follows: the diameter of catalyst particles was as small as possible, the porosity of catalyst particles packed decreased linearly along the radial direction from the centre of the tube, and the inflow mode was one-side in and one-side out.

However, most of the data sources for the existing models (Chein et al., 2010; Alagharu et al., 2010; Badescu, 2020; Xie et al., 2021) on NH_3 decomposition in tubular reactors directly extracted the experimental records in the literature, which may not be consistent with the CFD model design they adopted due to the lack of verification. To address this research gap, this study collected sufficient data from our group's experiment setup to establish and verify the CFD model construction. Furthermore, suitable correlations for NH_3 conversion and porosity and inlet gas temperature are provided that can be used as heuristics for scale-up experiments and future applications.

METHODOLOGY

Model configuration and assumptions

A two-dimensional fixed bed reactor model is used to clarify variations of concentration, velocity and temperature in the transverse and axial directions. This single-tube modelling method, which is a widely acknowledged idea in literature (Zeng et al., 2012), assumes that the intake distribution manifold will partition fluid equally. The reactor is a cylinder with a radius of D and a total length of L. Catalyst particles Ru/NiO catalyst are packed in the tube. A volumetric flow of room-temperature gaseous NH_3 is delivered into the reactor. An external heat source is used to heat the catalyst bed to the required reaction temperature T_w. In our model, D = 5.35 mm, L = 100 mm, and T_w= 500, 550, 600, 650, 700 °C. Due to the channel's symmetry, a half-width tube is taken into consideration for the simulation, as shown in Figure 1.

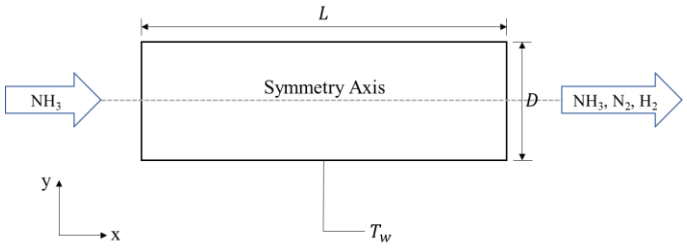

Figure 1 The two-dimensional fixed bed reactor model

With the conditions shown in Table 1, the analysis is simplified by the following assumptions:

(1) The flow is stable, axisymmetric and laminar because the Reynolds number (Reynolds, 1883) is 657 calculated by the following equation,

$$Re = \frac{\rho \vec{V} D}{\mu} \qquad (1)$$

in which Re, ρ, $\vec{V}$ and μ are Reynolds number, fluid density, velocity and viscosity respectively.

(2) The catalyst bed is modelled as a porous material with homogenous permeability κ and porosity ε, and the catalyst particles are treated as spherical with a diameter d_p.

(3) The catalysts and the surrounding gas mixture are in local thermal equilibrium.

(4) The gas mixture is considered an ideal gas since the specific heat of NH_3, N_2 and H_2 are all nearly constant within the considered temperature range.

Table 1 Geometric parameters and operating conditions

Reactor radius, D	5.35 mm
Reactor length, L	100 mm

NH_3 flow rate, F	900 mL/min
Wall temperature, T_w	500, 550, 600, 650, 700 °C
Inlet gas temperature, T_{in}	27 °C
Catalyst porosity, ε	0.698
Catalyst particle size, d_p	0.2875 mm

Governing equations

According to the Navier-Stokes equation (Phanikumar et al., 2002), the continuity equation for the laminar flow can be written as,

$$\nabla \cdot (\varepsilon \rho \vec{v}) = 0 \qquad (2)$$

in which, ε, ρ, $\vec{v}$ are porosity, fluid density and velocity respectively. Since the reactor tube is filled with porous catalyst, the Brinkman–Forchheimer equation is conducted to describe the pressure drop and flow velocity through the porous region (Mohammadi et al., 2020). Accordingly, the momentum conservation law can be presented as follows,

$$\nabla \cdot (\frac{\rho}{\varepsilon}\vec{v}\vec{v}) = -\nabla p + \nabla \cdot (\mu \nabla \vec{v}) - \frac{\mu \varepsilon}{\kappa}\vec{v} - \frac{\rho \varepsilon C_F}{\sqrt{\kappa}}|\vec{v}|\vec{v} \qquad (3)$$

where C_F, p, μ, κ represent the Forchheimer drag coefficient, pressure, viscosity and permeability.

The Navier-Stokes equation (Phanikumar et al., 2002) is used to model the fluid flow inside the reactor filled with porous catalysts. The porosity and the permeability are two key factors that govern mass transfer, heat transfer and fluid flow. The permeability of the porous region can be defined by the Carman-Kozeny model (Kaviany et al., 1995) as,

$$\kappa = \frac{d_p^2 \varepsilon^3}{150(1-\varepsilon)^2} \qquad (4)$$

As for the fluid density, the reactants and products are all gases thus the internal gas is considered the ideal gas mixture and is dominated by the ideal-gas mixing law. So the mass-weighted density ρ can be written as,

$$\rho = \frac{p}{RT}\sum_{i=1}^{N} x_i M_i \qquad (5)$$

In which, x_i, and M_i are the molar fraction and molecular weight of the ith species in the gas mixture, respectively. While the dynamic viscosity μ of the gas mixture and molecular diffusivity of the ith species D_i can be estimated based on Wilke's method (Poling et al., 2001) for the multi-component gas mixture as shown below,

$$\mu = \sum_{i=1}^{M} \frac{x_i \mu_i}{\sum_{j=1}^{N} x_j \phi_{ij}} \qquad (6)$$

$$D_i = \sum_{i=1}^{M} \frac{1 - x_i}{\sum_{j=1, j \neq i}^{N} \frac{x_j}{D_{ij}}} \qquad (7)$$

where μ_i is the viscosity of the ith species given as,

$$\mu_i = 2.67 \times 10^{-6} \frac{\sqrt{M_i T}}{\sigma_i^2 \Omega_{\mu,i}} \qquad (8)$$

where σ_i is the collision diameter of the ith species and $\sigma_{ij} = 1/2(\sigma_i + \sigma_j)$, $\Omega_{\mu,i}$ is the collision integrals for viscosity, and D_{ij} and ϕ_{ij} are the binary diffusivity and Chapman-Enskog parameter defined as,

$$D_{ij} = 1.86 \times 10^{-7} \frac{\sqrt{T^3 (\frac{1}{M_i} + \frac{1}{M_j})}}{p \sigma_{ij}^2 \Omega_{D,ji}} \qquad (9)$$

$$\phi_{ij} = \frac{[1 + (\mu_i/\mu_j)^{1/2} (M_i/M_j)^{1/4}]^2}{[8(1 + (M_j/M_i))]^{1/2}} \qquad (10)$$

in which, $\Omega_{D,ij}$ is the collision integral for binary diffusion.

Chemical processes (NH_3 decomposition) and the Joule effect (converting electrical energy to thermal energy) are included when discussing the various heat produced (or consumed) during the process. Calculations of the heat produced (or needed) for the different operations are conducted assuming perfect insulation. The model adopts the following equation to describe the heat transfer,

$$\rho C_p \vec{v} \cdot \nabla T = \nabla (k \nabla T) + Q \qquad (11)$$

In order to determine the heat capacity and the thermal conductivity for the decomposition side, the Chapman-Enskog theory is conducted as follows,

$$C_p = \sum_i C_{p_i} \cdot x_i \qquad (12)$$

$$\lambda = \sum_{i=1}^{N} \frac{x_i \lambda_i}{\sum_{j=1}^{N} x_i \phi_{ij}} \quad (13)$$

where λ_i is the conductivity of the ith species given as,

$$\lambda_i = 8.32 \times 10^{-2} \frac{\sqrt{T/M_i}}{\sigma_i^2 \Omega_{\lambda,i}} \quad (14)$$

in which, $\Omega_{\lambda,i}$ is the collision integral for thermal conductivity.

Boundary conditions

Boundary conditions must be specified to complete the mathematical model. Referring to Figure 1, the boundary conditions are specified as follows,

(i) Inlet ($x = 0$)

$$u = u_{in}, v = 0, T = T_{in} \quad (15)$$

$$c_{NH_3} = c_{NH_3,in}, c_{N_2,in} = 0, c_{H_2,in} = 0 \quad (16)$$

(ii) Outlet ($x = L$)

$$\frac{\partial \vec{v}}{\partial x} = \frac{\partial \mathrm{T}}{\partial x} = \frac{\partial C_i}{\partial x} = 0 \quad (17)$$

(iii) At the wall of the reactor ($y = D$)

$$\vec{v} = 0, T = T_{\mathrm{w}}, \frac{\partial C_i}{\partial \mathrm{y}} = 0 \quad (18)$$

(iv) Along the centreline ($y = 0$)

$$\frac{\partial \vec{v}}{\partial \mathrm{y}} = \frac{\partial \mathrm{T}}{\partial \mathrm{y}} = \frac{\partial C_i}{\partial \mathrm{y}} = 0 \quad (19)$$

Where T_{in}, c_{NH_3} and u_{in} are the temperature, molar concentration of NH_3, and inlet velocity respectively. They are specified by the Neumann boundary conditions for the outlet side, while the no-slip boundary condition is conducted on the wall. Assuming that no species deposits on the wall and the internal gas temperature is equal to the wall temperature.

Chemical reaction model

The decomposition of NH_3 is an endothermic reaction, and its stoichiometric decomposition reaction is expressed as,

$$NH_3 \rightleftharpoons \frac{1}{2} N_2 + \frac{3}{2} H_2 \quad (20)$$

The Arrhenius equation can be used to explain the general chemical reaction rate as follows,

$$r = A e^{-\frac{E_a}{RT}} (c_{NH_3})^{\alpha} (c_{N_2})^{\beta} (c_{H_2})^{\gamma} \quad (21)$$

where, r, A, E_a, and c_{NH_3} are the NH_3 decomposition rate, pre-exponential factor, activation energy and NH_3 molar concentration, respectively. α, β and γ represent the reaction order of NH_3, N_2 and H_2, respectively.

The catalyst adopted in this study is 1%Ru/NiO which has been reported in previous studies by our group (Zhai et al., 2023). To get the above kinetic parameters of the catalyst, experimental kinetic testing was conducted using the setup as shown in Figure 2a. To measure the catalytic NH_3 decomposition performance of designed catalysts, inside a quartz tube (diameter of 4.5 mm), c.a. 50 mg sieved (45-80 mesh) sample was sandwiched between two layers of quartz wool with a thermocouple placed in contact with the sample. Then high-purity NH_3 ($\geqslant$ 99.99%) was passed through the catalyst bed with the flow rate controlled by a mass flow controller. The weight hourly space velocity (WHSV) was set as 30,000 mL g cat^{-1} h^{-1} at atmospheric pressure. The concentrations of outlet N_2, H_2 and NH_3 after the reaction were measured online by MS (HPR-20 EGA, Hiden), which was equipped with a quadrupole probe and a secondary electron multiplier detector (850 eV). The accuracy of product analyses was further verified by back titration. The experimental details of the back titration methods have been reported in previous studies by our group (Zhai et al., 2023). The measured temperatures range from 200 to 500 °C with 50 °C as an interval, and a steady state was reached by maintaining each temperature for 60 min. The reaction orders were conducted by varying one gas concentration of N_2, H_2 or NH_3 with Ar as the balance gas and measured at 450 °C,

The NH_3 conversion was calculated using the following equation,

$$\mathrm{NH_3}\ conversion = \frac{[\mathrm{NH_3}]_{inlet} - [\mathrm{NH_3}]_{outlet}}{(1 + [\mathrm{NH_3}]_{outlet}) \times [\mathrm{NH_3}]_{inlet}} \times 100\% \quad (22)$$

where $[NH_3]_{inlet}$ and $[NH_3]_{outlet}$ refer to the measured concentrations of NH_3 fed into and flowing out of the reactor.

The Arrhenius plots (Figure 2b) and activation energies (Figure 2c) for NH_3 decomposition were calculated based on the activity evaluated under the same gas flow and compositions but at different temperatures with the conversion kept below 30%, so they were far from equilibrium.

The kinetic study indicates that the activation energy E_a of 1%Ru/NiO is 80.64 kJ/mol. This value is comparable to those previously reported for the Ru-based catalysts (60-120 kJ/mol) (Egawa et al., 1984; Hayashi et al., 2013; Di Carlo et al., 2014; Cerrillo et al., 2022). The reaction order of NH_3, N_2, and H_2 are 0.76, 0.03, and -1.75 respectively. The pre-exponential factor A is estimated to be 10^{10}.

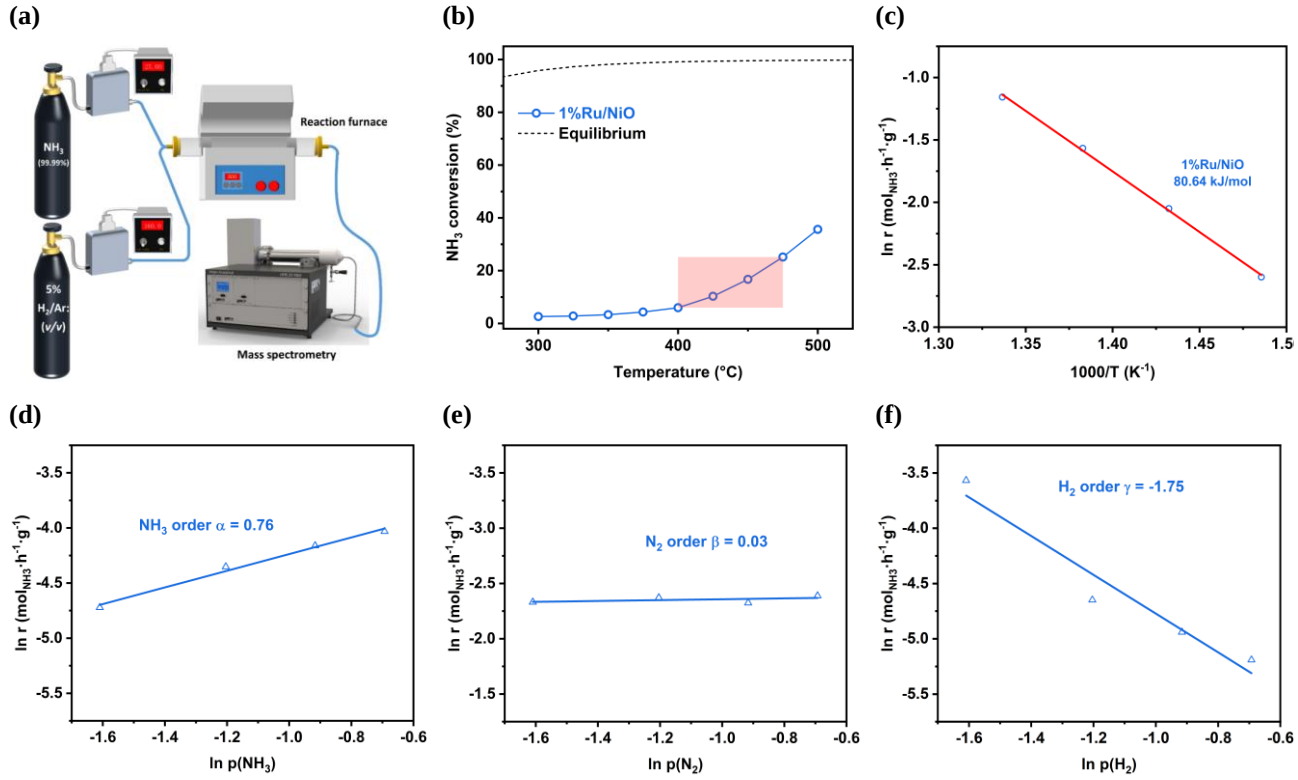

Figure 2 Catalytic performance tests for NH_3 decomposition. (a) Schematic of the kinetics studies setup; (b) NH_3 conversion as a function of reaction temperature; (c) activation energy; reaction order of (d) NH_3, (e) N_2 and (f) H_2.

Numerical model

Employing the commercial simulation software ANSYS Fluent version 2022R1, all of the theoretical equations are computed simultaneously. An imperative aspect of CFD simulations is the evaluation of grid dependency (Wibowo et al., 2019). The flow velocity at the outlet and pressure drop with different mesh cells are shown in Figure 3a. It is evident that the result is independent of the mesh structure when the cell number exceeds 60000. Therefore, the mesh configuration with 60000 cells is adopted in this numerical model. Figure 3b and Figure 3c show the pressure and temperature distribution contours inside the reactor model.

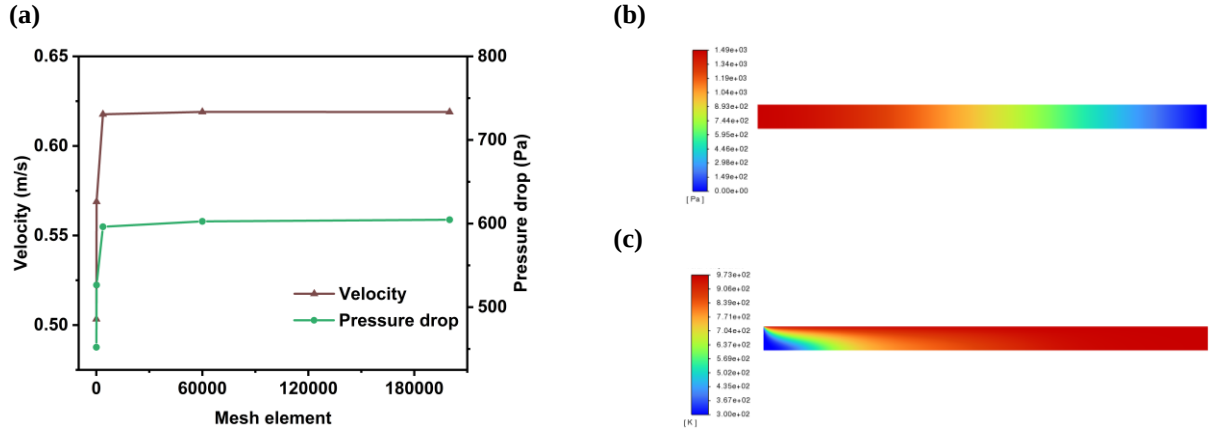

Figure 3 (a) Mesh independence study; (b) pressure and (c) temperature distribution

RESULTS AND DISCUSSION

Simulation validation and verification

In order to verify the feasibility of the numerical method, a series of experiments are conducted to make comparisons. A stainless steel tube is put in the centre of a furnace which is temperature-adjustable and electrically heated. A mass flow controller (D6341, Bronkhorst) regulates the amount of high-purity NH_3 gas that flows through the reactor tube. The activation and reaction processes both take place at atmospheric pressure. As NH_3 gas is extremely corrosive and dangerous, the corrosion resistance of all components used in its decomposition (pipes, mass flow controller, gas purifier, gas regulator, etc.) needs to be promised. When using NH_3 and the resulting H_2 as a fuel, it is important to have NH_3 and H_2 sensors installed in the areas where fuel lines are located, in addition to adequate ventilation. Fuel lines and Tanks should be equipped with remotely operable shut-off valves to isolate NH_3 and H_2 leakages and reduce their impact.

Under the existing experimental conditions, the tube's inner radius and length are 5.35 mm and 100 mm, and the 1%Ru/NiO catalyst particles are treated as spheres with a diameter of 0.2875 mm. The operation conditions of the experiment are set as follows: high-purity NH_3 flow of 900 mL/min, operating temperate from 500 to 700 °C with a 50 °C interval, and temperature of inlet NH_3 is 27 °C. The outlet gases were analyzed and confirmed by a mass spectrometer (Hiden Analytical HPR-20). The NH_3 conversion can be calculated by Equation 22.

Since NH_3 conversion is a direct and intuitive factor to describe the system performance and can be accessed conveniently both in simulation and experiment, its computational and experimental results will be compared to validate and demonstrate the reliability of the model. Under the same conditions including the reactor design, catalyst packing, and environmental setting, to run the model and operate the experiment respectively. The results are shown in Figure 4a. The growth trend of the conversion rates with wall temperatures varies from 500 to 700 °C are very similar. The deviation between experiment and simulation results are 35%, 5%, 1%, 0 and 0 when T_w = 500, 550, 600, 650, and 700 °C, respectively. This indicates that the two results match very well except for 500 °C, at which the model still needs further improvement. In general, the comparison result indicates a good agreement and hence shows that the numerical method in this paper is reasonable and applicable.

Influence of catalyst porosity

Porosity could vary depending on the packing arrangement, which will result in different packed bed permeability and Forchheimer drag coefficient. The variations of catalyst bed permeability and Forchheimer drag coefficient result in different gas mixture flow velocities and thus affect the NH_3 decomposition using the above verified numerical model. Therefore, this paper studies extensively the relationship between NH_3 decomposition performance and particle porosity. As shown in Figure 4b, the porosity effects on the NH_3 decomposition are presented under the 900 mL/min flow rate for various reaction temperatures. It is clear that the NH_3 conversion rises with the increase of the porosity from 0.2 to 0.8. The reason is that higher porosity leads to a decrease in the resistance along the flowing direction in the tube, which is advantageous to the reaction. In addition, with the increase of porosity, the contact area of gas and catalyst increases which results in an enhancement of NH_3 decomposition.

Influence of inlet gas temperature

Apart from the effect of the fluid flow, the temperature influence also dominates the reaction processes, so it is necessary to investigate the temperature effect. In this study, the influence of inlet gas temperature on NH_3 decomposition is analyzed with the help of the theoretical model, as shown in Figure 4c. If preheating the inlet NH_3 flow to the target temperature, namely the wall temperature, the reaction can be significantly enhanced. The improvements through preheating are especially significant for low temperatures situations. For example, NH_3 conversion increases by 81.5% and 36.0% respectively at T_w = 550 °C and 600 °C. Thus, heating NH_3 to the desired temperature before the inlet can help to optimize the reactor performance. However, the preheating of reactants before the inlet side certainly will increase the economic cost (extra energy input). Both these two factors should be taken into consideration before evaluating the need for preheating. This result offers valuable theoretical references for future experiments.

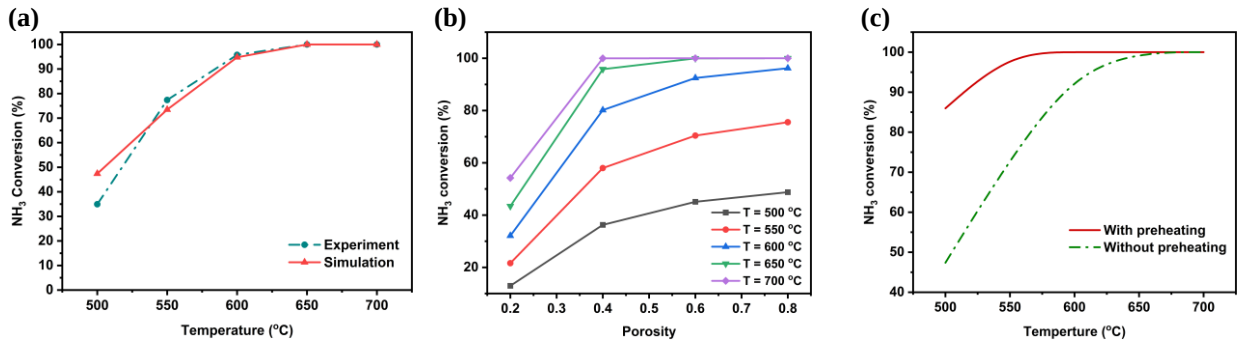

Figure 4 (a) Comparison between the simulation results and experiment data; (b) variation of NH_3 conversion rate with porosity and temperatures; (c) effect of inlet gas temperature on NH_3 conversion.

CONCLUSIONS

A two-dimensional model of H_2 production via NH_3 decomposition in a tubular catalyst-packed bed is established to simulate the reaction system with the support of experiment data. The relation between NH_3 conversion rate and operating parameters including porosity and inlet gas temperature are analyzed. The increase of catalyst porosity and the preheating of inlet NH_3 are both beneficial to NH_3 conversion. It is achieved that the preheating of inlet gas resulted in an 81.5% improvement in conversion when the temperature is 500 °C. This study has offered theoretical guidelines for experiment design and applications. However, there are some deficiencies in the investigation and more research work on parameter sensitivity and system optimization should be devoted in the future. For example, the impact of the tube diameter and catalyst particle size should be included when analyzing porosity influence. Moreover, for practical applications, scale-up simulations based on reliable experiment data configuration design are necessary. Therefore, further investigation on simulation in large-scale NH_3 reactions with a two-dimensional or even three-dimensional model should be presented in future work.

NOMENCLATURE

D	Reactor Radius
L	Reactor length
d_p	Catalyst particle diameter
T_{in}	Inlet gas temperature
T_w	Wall temperature
ρ	Fluid density
$\vec{v}$	Velocity
μ	Viscosity
p	Pressure
ε	Porosity
κ	Permeability
λ	Thermal conductivity
C_p	Heat capacity
R	Reaction rate
E_a	Activation energy
A	Pre-exponential factor
α	Reaction order of NH_3
β	Reaction order of N_2
γ	Reaction order of H_2

ACKNOWLEDGMENTS

This work was financially supported by the Hong Kong Polytechnic University (P0043756) and the Innovation and Technology Fund of Hong Kong (ITS/077/21).

References

ANSYS Fluent 2022R1 User's Guide. Lebanon, USA: Fluent Inc.

Alagharu, V., Palanki, S. & West, K. N. (2010). Analysis of ammonia decomposition reactor to generate hydrogen for fuel cell applications. *Journal of Power Sources*, 195**,** 829-833. https://doi.org/10.1016/j.jpowsour.2009.08.024

Badescu, V. (2020). Optimal design and operation of ammonia decomposition reactors. *International Journal of Energy Research*, 44**,** 5360-5384. https://doi.org/10.1016/j.jpowsour.2009.08.024
Cerrillo, J. L., Morlanés, N., Kulkarni, S. R., Realpe, N., Ramírez, A., Katikaneni, S. P., Paglieri, S. N., Lee, K., Harale, A. & Solami, B. (2022). High purity, self-sustained, pressurized hydrogen production from ammonia in a catalytic membrane reactor. *Chemical Engineering Journal*, 431**,** 134310. https://doi.org/10.1016/j.cej.2021.134310
Chang, F., Gao, W., Guo, J. & Chen, P. (2021). Emerging materials and methods toward ammonia‐based energy storage and conversion. *Advanced Materials*, 33**,** 2005721. https://doi.org/10.1002/adma.202005721
Chein, R.-Y., Chen, Y.-C., Chang, C.-S. & Chung, J. (2010). Numerical modeling of hydrogen production from ammonia decomposition for fuel cell applications. *International Journal of Hydrogen Energy*, 35**,** 589-597. https://doi.org/10.1016/j.ijhydene.2009.10.098
Deng, Z., Hu, T., Tian, J. & Wang, Y. (2020). Performance of a novel single-tubular ammonia-based reactor driven by concentrated solar power. *Solar Energy*, 204**,** 696-707. https://doi.org/10.1016/j.solener.2020.04.081
Di Carlo, A., Vecchione, L. & Del Prete, Z. (2014). Ammonia decomposition over commercial Ru/Al_2O_3 catalyst: An experimental evaluation at different operative pressures and temperatures. *International Journal of Hydrogen Energy*, 39**,** 808-814. https://doi.org/10.1016/j.ijhydene.2013.10.110
Egawa, C., Nishida, T., Naito, S. & Tamaru, K. (1984). Ammonia decomposition on (1 1 10) and (0 0 1) surfaces of ruthenium. *Journal of the Chemical Society, Faraday Transactions 1: Physical Chemistry in Condensed Phases*, 80**,** 1595-1604. https://doi.org/10.1039/F19848001595
Giorgi, L., Salernitano, E., Makris, T. D., Gagliardi, S., Contini, V. & De Francesco, M. (2014). Innovative electrodes for direct methanol fuel cells based on carbon nanofibers and bimetallic PtAu nanocatalysts. *International Journal of Hydrogen Energy*, 39**,** 21601-21612. https://doi.org/10.1016/j.ijhydene.2014.06.053
Hayashi, F., Toda, Y., Kanie, Y., Kitano, M., Inoue, Y., Yokoyama, T., Hara, M. & Hosono, H. (2013). Ammonia decomposition by ruthenium nanoparticles loaded on inorganic electride $C_{12}A_7{:}e^-$. *Chemical Science*, 4**,** 3124-3130. https://doi.org/10.1039/C3SC50794G
Kaviany, M. & Kaviany, M. (1995). Conduction heat transfer. *Principles of Heat Transfer in Porous Media***,** 119-156.
Mohammadi, M. H., Abbasi, H. R., Yavarinasab, A. & Pourrahmani, H. (2020). Thermal optimization of shell and tube heat exchanger using porous baffles. *Applied Thermal Engineering*, 170**,** 115005. https://doi.org/10.1016/j.applthermaleng.2020.115005
Phanikumar, M. & Mahajan, R. (2002). Non-darcy natural convection in high porosity metal foams. *International Journal of Heat and Mass Transfer*, 45**,** 3781-3793. https://doi.org/10.1016/S0017-9310(02)00089-3
Poling, B. E., Prausnitz, J. M. & O'connell, J. P. (2001). *Properties of gases and liquids*, McGraw-Hill Education.
Pourali, M., Esfahani, J. A., Jahangir, H., Farzaneh, A. & Kim, K. C. (2022). Ammonia decomposition in a porous catalytic reactor to enable hydrogen storage: numerical simulation, machine learning, and response surface methodology. *Journal of Energy Storage*, 55**,** 105804. https://doi.org/10.1016/j.est.2022.105804
Reynolds, O. (1883). An experimental investigation of the circumstances which determine whether the motion of water shall be direct or sinuous, and of the law of resistance in parallel channels. *Philosophical Transactions of the Royal society of London***,** 935-982. https://doi.org/10.1098/rstl.1883.0029
Takahashi, A. & Fujitani, T. (2021). Kinetic-model-based design of industrial reactor for catalytic hydrogen production via ammonia decomposition. *Chemical Engineering Research and Design*, 165**,** 333-340. https://doi.org/10.1016/j.cherd.2020.11.004
Wibowo, S. B. & Rohmat, T. A. (2019). Study of mesh independence on the computational model of the roll-up vortex phenomenon on fighter and delta wing models. *International Journal of Fluid Mechanics Research*, 46. https://doi.org/10.1615/InterJFluidMechRes.2018025530
Xie, T., Xia, S. & Wang, C. Multi-objective performance optimization of ammonia decomposition thermal storage reactor. E3S Web of Conferences, 2021. EDP Sciences, 02073. https://doi.org/10.1051/e3sconf/202126702073
Zeng, D., Pan, M. & Tang, Y. (2012). Qualitative investigation on effects of manifold shape on methanol steam reforming for hydrogen production. *Renewable Energy*, 39**,** 313-322. https://doi.org/10.1016/j.renene.2011.08.027
Zhai, L., Wong, C. S., Zhang, H., Xiong, P., Xue, X., Ho, Y. L., Xu, C., Fong, Y. C., Mei, J. & Chan, W. W. (2023). From lab to practical: An ammonia-powered fuel cell electric golf cart system. *Chemical Engineering Journal*, 452**,** 139390. https://doi.org/10.1016/j.cej.2022.139390